

CONTAMINANT TRANSPORT IN DUAL-WELL FLOW

B. MALENGIER * AND J. KAČUR †

Abstract. We present a new solution for contaminant transport in dual-well flow. The numerical approximation is based on a dipol transformation of a convection-diffusion model for the contaminant transport in a finite rectangular domain with stream lines parallel to one of the axis. The transport and the diffusion part are split along the time intervals. The transport is reduced to the solution of a multiple Riemann problem with semi-analytic solution. The numerical experiments are compared in a specific case with the semi-analytical solution.

Key words. convection-diffusion equations, operator splitting methods, method of characteristics.

AMS subject classifications. 65PO5, 76R99, 76SO5

1. Introduction. Contaminant transport with adsorption is a very dynamical and difficult research area. Precise mathematical models are available, and a big effort has been done to develop effective mathematical tools to obtain a desired solution. In practical implementations the precise physical data in the model are required (hydrodynamical and geophysical). Some of them can be obtained only in authentic fields, where these models will be applied. The diffusion part of the model is generated by dispersivity properties of the considered porous media, where the contaminant transport is considered. The dispersivity properties are characterized by longitudinal α_L and transversal α_T coefficients. Their determination (calibration of the model) can be realized by dual-well tests with a steady state flow regime. In one of the wells the water is injected and in the other one it is extracted. In the injection well we can implement a tracer and then at the extraction well we measure the response in the form of the time evolution of the extracted tracer (break through curves (BTC)). From the shape of the BTC we can restore the corresponding parameters α_L , α_T under the assumption that other datas of the model are known.

For the flow model we use the Dupuit-Forchheimer approximation leading to a two dimensional flow in an aquifer. We also use the assumption that the porous medium is homogeneous. On the other hand we do not assume that the aquifer is confined as it is done in many other approximate models. We assume that in the neighbourhood of the injection well the aquifer is confined, while in a neighbourhood of the extraction well it is unconfined.

2. Mathematical model. The steady state flow, under the Dupuit-Forchheimer approximation (see [H]), is governed by the elliptic equation

$$\Delta\Phi = 0, \quad \text{in } \mathbb{R}^2 \setminus B_{r_1}(-d, 0) \cup B_{r_2}(d, 0), \quad (2.1)$$

($B_r(x, y)$ denotes a ball with the radius r and the center (x, y)), with the boundary conditions

$$\Phi = \Phi_1 \quad \text{on } \partial B_{r_1}, \quad \Phi = \Phi_2 \quad \text{on } \partial B_{r_2}. \quad (2.2)$$

*Department of Mathematical Analysis, Ghent University, Building S-22, Galglaan 2, B-9000 Ghent, Belgium. E-mail: bm@cage.rug.ac.be

†Faculty of Mathematics and Physics, Comenius University Bratislava, Mlynská dolina, 84215 Bratislava, Slovakia. E-mail: kacur@fmph.uniba.sk

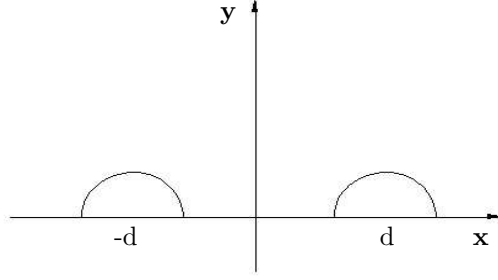


FIG. 2.1. Boundary of the domain Ω in (x, y) coordinates. Injection well $x = d$, extraction well at $x = -d$.

Here, Φ denotes the flow potential, r_1 and r_2 are the well diameters, and d is half the distance between the wells. The flow potential in the (unbounded) aquifer of height H , relates to the pressure-head $h = h(x, y)$, namely

$$\Phi(x, y) = khH - \frac{1}{2}kH^2, \quad \text{if } \Phi \geq \frac{1}{2}kH^2 \quad (2.3)$$

$$\Phi(x, y) = \frac{1}{2}kh^2, \quad \text{if } \Phi \leq \frac{1}{2}kH^2, \quad (2.4)$$

where k is the hydraulic permeability. The curve $\sqrt{\frac{2\Phi(x, y)}{k}} = H$ (Φ is a solution of (2.1), (2.2)) separates the confined and unconfined zones. Due to the symmetry along the x -axis, we solve (2.1) and (2.2) only in the upper half plane, see Fig. 2.1

The transport equation for a tracer, C , has the form - see [B]

$$h_{eff}\partial_t C = \text{div}(Dh_{eff}\nabla C) - \text{div}(h_{eff}\bar{v}C), \quad (2.5)$$

where D is the dispersivity tensor

$$D_{ij} = \left\{ (D_0 + \alpha_L |v|)\delta_{ij} + \frac{v_i v_j}{|v|}(\alpha_T - \alpha_L) \right\},$$

$h_{eff} := \min \{h, H\}$, and

$$\bar{v} = -\frac{1}{h_{eff}\theta_0}\nabla\Phi,$$

where θ_0 is the porosity.

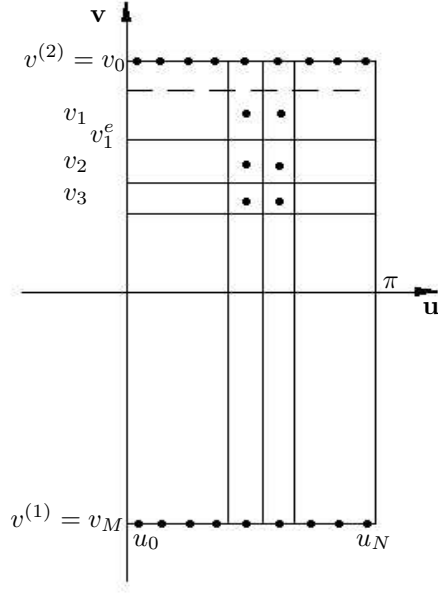
A precise solution of (2.1-2.5) is required to determine α_L , α_T (inverse problem).

3. Method of solution. Problem (2.1), (2.2) can be efficiently solved using a conformal mapping (see [C-K]). This leads to a bipolar transformation of Ω to $\tilde{\Omega} \equiv (0, \pi) \times (v^{(1)}, v^{(2)})$ - see Fig 3.1 - with new variables u , v given by

$$x = \frac{\delta}{2} \frac{\sinh v}{\cosh v - \cos u}, \quad y = \frac{\delta}{2} \frac{\sin u}{\cosh v - \cos u},$$

where we obtain δ from

$$\sqrt{r_1^2 + \frac{1}{4}\delta^2} + \sqrt{r_2^2 + \frac{1}{4}\delta^2} = 2d, \quad (2d > r_1 + r_2).$$

FIG. 3.1. Boundary of the domain $\tilde{\Omega}$ in (u, v) coordinates.

Then $\tilde{\Phi}(u, v) = \Phi(x, y)$ depends only on v -variable, since the streamlines and the equipotential curves of Φ create the lines parallel with (u, v) -axes. The values $v^{(1)}$, $v^{(2)}$ are obtained from

$$\sinh v^{(1)} = -\frac{\delta}{2r_1} \quad \sinh v^{(2)} = \frac{\delta}{2r_2}.$$

Then $\tilde{\Phi}(u, v) = Av + B$, where A, B are determined by the boundary conditions (2.2). It holds

$$Av^{(1)} + B = \Phi_1 \equiv \frac{1}{2}kh_1^2, \quad Av^{(2)} + B = \Phi_2 \equiv kh_2H - \frac{1}{2}kH^2,$$

in the assumption that B_{r_1} is the extraction well and $h_1 < H$. We can identify the pressure-head with the water level (the stratum is the bottom of aquifer). In the injection well we have the water level $h_2 > H$. Other possibilities, e.g. $H < h_1 < h_2$; $h_1 < h_2 < H$, can also be included.

Applying the same transformation to the contaminant transport equation (2.5), gives (see [C-K]):

(i) for $h > H$,

$$\begin{aligned} \partial_t C = \frac{4\lambda^2}{\delta^3\theta_0 H} \left\{ \partial_u \left[\left(D_0\theta_0 H\delta + 2\alpha_T\lambda(\partial_v\tilde{\Phi}(v)) \right) \partial_u C \right] + \right. \\ \left. + \partial_v \left[\left(D_0\theta_0 H\delta + 2\alpha_L\lambda(\partial_v\tilde{\Phi}(v)) \right) \partial_v C + \delta(\partial_v\tilde{\Phi}(v))C \right] \right\}, \end{aligned} \quad (3.1)$$

(ii) for $h \leq H$,

$$\begin{aligned} \partial_t C = \frac{4\lambda^2}{\delta^3\theta_0 h(v)} \left\{ \partial_u \left[\left(D_0\theta_0 h(v)\delta + 2\alpha_T\lambda(\partial_v\tilde{\Phi}(v)) \right) \partial_u C \right] + \right. \\ \left. + \partial_v \left[\left(D_0\theta_0 h(v)\delta + 2\alpha_L\lambda(\partial_v\tilde{\Phi}(v)) \right) \partial_v C + \delta(\partial_v\tilde{\Phi}(v))C \right] \right\}, \end{aligned} \quad (3.2)$$

where $\lambda = \cosh v - \cos u$ and $\partial_v \tilde{\Phi}(v) = A$.

We write (3.1), (3.2) in the form

$$\partial_t C - K\lambda^2 \partial_v C = g \{ \partial_u(a(u, v)\partial_u C) + \partial_v(b(u, v)\partial_v C) \}, \quad (3.3)$$

and consider the boundary conditions

$$C = C_0(t) \text{ on } \Gamma_1; \quad \partial_u C = 0 \text{ on } \Gamma_2 \cup \Gamma_4; \quad \partial_v C = 0 \text{ on } \Gamma_3, \quad (3.4)$$

where $\Gamma_1 := (0, \pi) \times \{v = v^{(2)}\}$, $\Gamma_2 := \{0\} \times (v^{(1)}, v^{(2)})$, $\Gamma_3 := (0, \pi) \times \{v^{(1)}\}$ and $\Gamma_4 := \{\pi\} \times (v^{(1)}, v^{(2)})$, together with the homogeneous initial condition

$$C((u, v), 0) = 0. \quad (3.5)$$

The function $C_0(t)$ is either a constant ($C_0(t) = C^0$) or a pulse shape, or piecewise constant.

To solve the convection diffusion problem we use timestepping and operator splitting in which, along any small time interval, the problem is splitted into 2 parts: *the transport problem* and *the diffusion problem*. More in details, let $\tau = T/n$ be a time step and $C_i \approx C((u, v), t_i)$ for $i = 1, \dots, n$. Given C_{i-1} the relation

$$C_i = D^i(\tau)T^i(\tau)C_{i-1}, \quad \tau = t_i - t_{i-1},$$

determines C_i . The transport $T^i(\tau)$ corresponds to the solution ϕ_T of the transport equation

$$\partial_t \phi - K\lambda^2 \partial_v \phi = 0, \quad (3.6)$$

with the inflow condition $\phi_T((u, v_2), t) = C_0(t)$ and the initial condition

$$\phi_T((u, v), t_{i-1}) = C_{i-1}.$$

The diffusion $D^i(\tau)$ is obtained by solving the diffusion equation

$$\partial_t \phi = g \{ \partial_u(a(u, v)\partial_u \phi) + \partial_v(b(u, v)\partial_v \phi) \}, \quad (3.7)$$

with the boundary conditions (3.4) and the initial condition $\phi((u, v), t_{i-1}) = C_{i-1}^{1/2}$.

Then we set

$$C_i^{1/2} := T^i(\tau)C_{i-1} \equiv \phi_T((u, v), t_i).$$

and

$$C_i = D^i(\tau)C_i^{1/2} = D^i(\tau)T^i(\tau)C_{i-1} \equiv \phi((u, v), t_i).$$

The solution of the transport problem (3.6) will be based on a piecewise constant initial profile C_{i-1} , i.e., solution of the multiple Riemann problem, which we can obtain precisely, in analytical form. The solution of (3.7) will be realized by the finite difference method, which in the discretization of our domain $\tilde{\Omega}$ (see §4 below) coincides with the FVM (finite volume method). The result will be again a piecewise constant function. Hence we can proceed analogously in the next time step.

4. Numerical approximation of equation (3.3). The space discretization is as follows. Let $\{u_i\}_{i=0}^N, \{v_j\}_{j=0}^M$ be nodal points, not necessarily equidistant, in u and v respectively. We have $v_0 = v^{(2)}, v_M = v^{(1)}$, so $v_0 > v_M$, and $0 < u_0 < u_N < \pi$, see Fig. 3.1. We define $\Delta u_+ = u_{i+1} - u_i$, $\Delta u_- = u_i - u_{i-1}$, $u_{i+1/2} = u_i + \Delta u_+/2$, $u_{i-1/2} = u_i - \Delta u_-/2$, $\Delta u = u_{i+1/2} - u_{i-1/2}$. Analogously for v , where e.g. $\Delta v_+ = v_{j-1} - v_j$. In this way we have u_i -strips defined by $(u_{i-1/2}, u_{i+1/2}) \times (v^{(1)}, v^{(2)})$, and in these strips elements defined by $(u_{i-1/2}, u_{i+1/2}) \times (v_{j+1/2}, v_{j-1/2})$ in which we have the node (u_i, v_j) . For the edges of $\tilde{\Omega}$ we set $u_{-1/2} \equiv 0$, $u_{N+1/2} \equiv \pi$, $v_{-1/2} \equiv v_0$ and $v_{M+1/2} \equiv v_M$.

4.1. Solution of the transport problem. We shall solve (3.6) in the strip $(u_{i_0-1/2}, u_{i_0+1/2}) \times (v^{(1)}, v^{(2)})$ with grid points $v_0^e \equiv v^{(2)}$, $v_1^e \equiv v_{3/2}$, $v_2^e \equiv v_{5/2}, \dots$, $v_{M-1}^e \equiv v_{M-1/2}$, $v_M^e \equiv v^{(1)}$. Let the initial profile be a piecewise constant function $\phi_0(v)$ with shocks in the grid points and denote $\phi_0(v) = U^j$ for $v \in (v_j^e, v_{j-1}^e)$. Transform (3.6) using the new variable $y = y(v)$ where

$$y = F(v) = \int_{v^{(1)}}^v \frac{dv}{K\lambda^2}, \quad \lambda^2 = (\cosh(v) - p_{i_0})^2, \quad p_{i_0} = \cos u_{i_0}.$$

Then $\bar{\phi}(y, t) = \phi(v, t)$ satisfies

$$\partial_t \bar{\phi} - \partial_y \bar{\phi} = 0, \quad \bar{\phi}(y, 0) = \phi_0(v).$$

Since λ is positive, the transformation is one to one. The solution can be written in the form

$$\bar{\phi}(y, t) = \bar{\phi}(y + t, 0), \quad \text{or} \quad \bar{\phi}(y, 0) = \bar{\phi}(y - t, t),$$

and, consequently, using the inverse $F^{-1} : y \mapsto v$, we obtain $\phi(v, t)$ from $\bar{\phi}(y, t)$. Notice that we need not make the inverse in all points y , since it follows that $\bar{\phi}(y, t)$ is piecewise constant with the values $\{U_j\}_{j=1}^N$. It is sufficient to compute first,

$$y_k = \int_{v^{(1)}}^{v_k^e} \frac{dx}{K\lambda^2}, \quad \text{for } k = 0, \dots, M,$$

then shift it over the timestep τ , and compute the inverse $F^{-1}(y_k - \tau) := \delta_k$ for $k = 0, \dots, M$. The solution $\phi(v, \tau)$ then attains the constant value $U^{j_k} \in \{U_j\}_{j=1}^N$ in the interval (δ_k, δ_{k-1}) . Recall that the direction of velocity is opposite to the direction of v -axes.

The final output, which will be used as input of the diffusion part (see §4.2), is obtained by projecting $\phi(v, \tau)$ to piecewise constants on intervals (v_j^e, v_{j-1}^e) , $j = 1, \dots, M$. This corresponds to take averages over (v_j^e, v_{j-1}^e) . For example, if $\delta_k \in (v_j^e, v_{j-1}^e)$ and $\delta_{k-1}, \delta_{k+1} \notin (v_j^e, v_{j-1}^e)$, then we have

$$C_l^{1/2}(v) = U^{j_k} \frac{v_{j-1}^e - \delta_k}{v_{j-1}^e - v_j^e} + U^{j_{k+1}} \frac{\delta_k - v_j^e}{v_{j-1}^e - v_j^e}, \quad \text{for } v \in (v_j^e, v_{j-1}^e),$$

and, similarly in other cases. E.g., if $v_{j-1}^e < \delta_{k-1} < v_{j-2}^e$ and $v_{j+1}^e < \delta_k < v_j^e$, then $C_l^{1/2}(v) = U^{j_k}$ for $v \in (v_j^e, v_{j-1}^e)$.

Then $C_l^{1/2} = PC^{1/2} = PT(\tau)$ is piecewise constant and we can switch to the diffusion.

Recall that in the confined setting ($h_2 > h_1 \geq H$), we can express $F(v)$ in an analytical form $F(v) = F(v; p) = (\overline{F}(v; p) - \overline{F}(v^{(1)}; p)) / K$ and

$$\overline{F}(v, p) := \frac{2pz - 2}{(1 - p^2)(z^2 - 2pz + 1)} + \frac{2p}{(1 - p^2)^{3/2}} \arctan \frac{z - p}{\sqrt{1 - p^2}} \quad (4.1)$$

where $z = e^v$, $p = \cos u_{i_0}$ (when we are in the strip $u_{i_0-1/2} < u < u_{i_0+1/2}$). In the unconfined setting, $F(v)$ must be determined numerically. To determine $\delta_k = F^{-1}(y_k - \tau)$ for $y_k - \tau \in (y_j, y_{j-1})$ so that $\delta_k \in (v_j^e, v_{j-1}^e)$, we use a Newton iteration. Namely, we look for the zero point of $\psi(v) \equiv F(v) - (y_k - \tau)$ starting from v_j where $\psi(v_j) = y_j - y_k + \tau$. Note that $\psi(v)$ and the derivative $\psi'(v) = \frac{1}{K\lambda^2}$ can be easily computed for every v .

4.2. Solution of the diffusion part. We use as grid points $\{u_i, v_j\}$, $i = 0, \dots, N$; $j = 1, \dots, M$. The diffusion part of (3.3) is

$$\partial_t \phi = g \{ \partial_u (a(u, v) \partial_u C) + \partial_v (b(u, v) \partial_v C) \}, \quad (4.2)$$

with boundary conditions (3.4).

We integrate (4.2) over (t_{k-1}, t_k) and $V_{ij} \equiv (u_{i-1/2}, u_{i+1/2}) \times (v_{j+1/2}, v_{j-1/2})$, and assume that $g_{ij} = g(u_i, v_j)$ is the prevailing value over V_{ij} . Denote $C^E \equiv C_{i,j}^E = C_{i+1,j}$, $C^W \equiv C_{i,j}^W = C_{i-1,j}$ and similarly C^N , C^S . We denote further $a^E = a_{ij}^E = a(u_{i+1/2}, v_j)$, $a^W = a_{ij}^W = a(u_{i-1/2}, v_j)$ and similarly b^N , b^S . Setting $\omega = \omega_{ij} = \frac{|V_{ij}|}{g_{ij}}$, gives the following linear algebraic system

$$\begin{aligned} & \left[\omega + \left(a^E \frac{\Delta v}{\Delta u_+} + a^W \frac{\Delta v}{\Delta u_-} + b^N \frac{\Delta u}{\Delta v_+} + b^S \frac{\Delta u}{\Delta v_-} \right) \tau \right] C_{i,j} = \quad (4.3) \\ & \left[\tau \frac{\Delta v}{\Delta u_-} a^W \right] C_{i-1,j} + \left[\tau \frac{\Delta v}{\Delta u_+} a^E \right] C_{i+1,j} \\ & + \left[\tau \frac{\Delta u}{\Delta v_+} b^N \right] C_{i,j+1} + \left[\tau \frac{\Delta u}{\Delta v_-} b^S \right] C_{i,j-1} + \omega C_{i,j}^{k-1}. \end{aligned}$$

Taking into account the boundary conditions (3.4) we have to put $a^W \equiv 0$ for the points $\{u_0, v_j\}$ and $a^E \equiv 0$ for the points $\{u_N, v_j\}$, $j = 1, \dots, N$. Moreover for $\{u_i, v_M\}$, $i = 0, \dots, N$ we take $b^S \equiv 0$ in (4.3).

The matrix corresponding to (4.3) is diagonal dominant and positive definite. For the solution we use a modified generalized conjugate residual algorithm method.

It is well known that the transversal dispersivity coefficient is one order smaller than the longitudinal (see [B]). As a consequence, we can put $\alpha_T = 0$ in (3.1), (3.2). If also $D_0 = 0$, the diffusion is reduced to only the v -direction ($a(u, v) = 0$). Then a simple TDMA (tridiagonal matrix algorithm, see [P]) can be used to solve in each strip one dimensional diffusion. The convergence of the used approximation is based on convergence results for operator splitting approximation, see [C-M], [K-L], etc.

5. Numerical experiments. We compare our results with those obtained by C.Welly and L.W. Gelhar in [W-G]. The mentioned authors used a simplified mathematical model which is based on the analytical expressions for streamlines and equipotential curves for point sources (injection and extraction). Their model violates the Dupuit-Forchheimer assumptions in the neighbourhood of point sources. On the other hand they obtained a semi-analytical solution, which avoids numerical dispersion. Our numerical dispersion arises when we project the solution after transport,

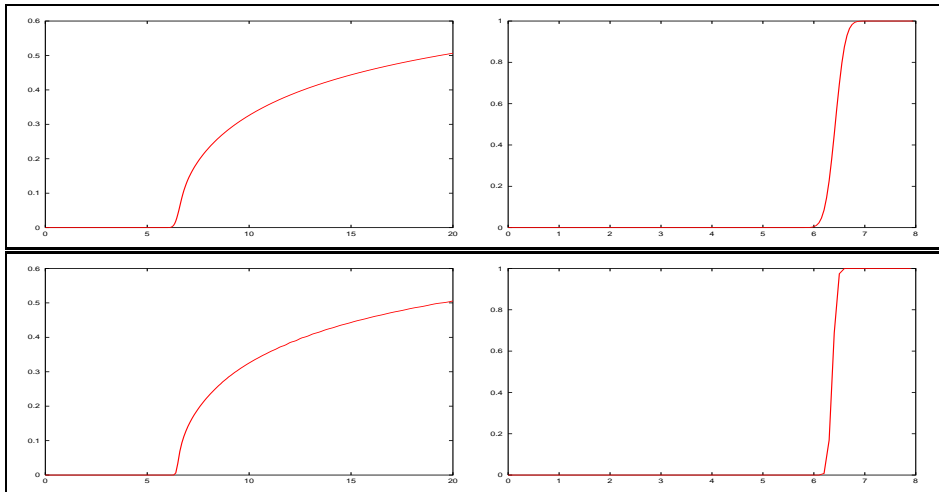


FIG. 5.1. *BTC for the transport problem, horizontal axis: time in days, vertical axis: relative concentration C/C_0 . Upper part: timestep = 0.05 day, grid 80×200 . Lower part: timestep = 0.1 day, grid 80×400 . To the left: the BTC for a step input. To the right: the BTC for the u_N strip, corresponding to the line connecting the two wells (x -axis).*

to piecewise constant function with respect to the used discretization. As a remedy, one could change the mesh after each transport in time interval (t_{k-1}, t_k) , $k = 1, \dots$, but this would be numerically costly.

Our approximation keeps local and global mass balance. If we neglect D_0 , α_L , α_T (i.e. diffusion), the response of contaminant injection at $t = 0$ is expected exactly at time T_r

$$y_0 - T_r = y_N, \text{ i.e. } T_r = \int_{v^{(1)}}^{v^{(2)}} \frac{dv}{K\lambda^2}, \quad (5.1)$$

for $u = \pi$, or $p = -1$, which corresponds to the line connecting the centers of the wells. This time of responds should correspond to the beginning of a withdrawal curve corresponding to the pulse type injection of contaminant. This characteristic also can be used to measure the quality of the numerical solution.

Furthermore, we compare the shape of the BTC with constant inflow condition, and also with pulse type inflow, with the one obtained in [W-G].

5.1. Experiment 1. We investigate the convergence and the numerical dispersion of the method. Consider the following data: both wells have a radius of $r_1 = r_2 = 15\text{cm}$, and their centers are placed 10m ($d = 5\text{m}$) from each other. The height of the aquifer is $H = 10\text{m}$, and the prescribed head value is $h_1 = 10\text{m}$ at the extraction well, $h_2 = 15\text{m}$ at the injection well (confined flow). The porosity of the soil is $\theta_0 = 0.2$, the hydraulic conductivity $k = 0.864\text{m}^2/\text{day}$. Since the numerical dispersion arises from the projection after transport, we consider only the transport problem, so $\alpha_L = \alpha_T = 0$. Moreover, for the grid we take an equidistant u partition ($\Delta u = \pi/(N + 1)$, $u_0 = \pi/(2(N + 1))$), and a non-equidistant v partition deduced from an equidistant x partition along the x -axis between the two wells.

As the BTC corresponds with the responds over all flow-lines, we also depict the BTC of the u_N strip, the shortest path between the wells, which should be equal to the input concentration delayed by T_r . In Fig. 5.1 the BTC for a step input starting

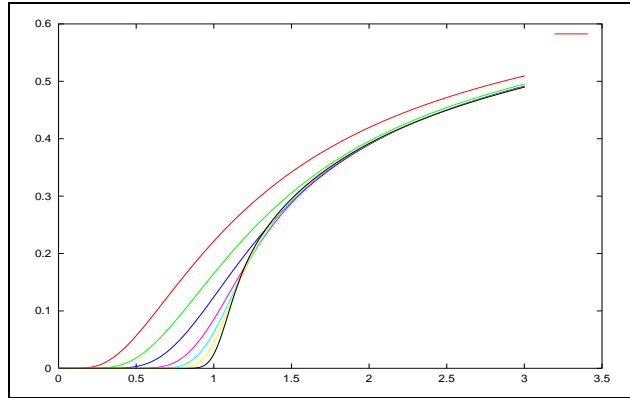


FIG. 5.2. Scaled BTC with pulse input for $\alpha_L/L = 0.2, 0.1, 0.05, 0.02, 0.01, 0.005$ and 0.002 .

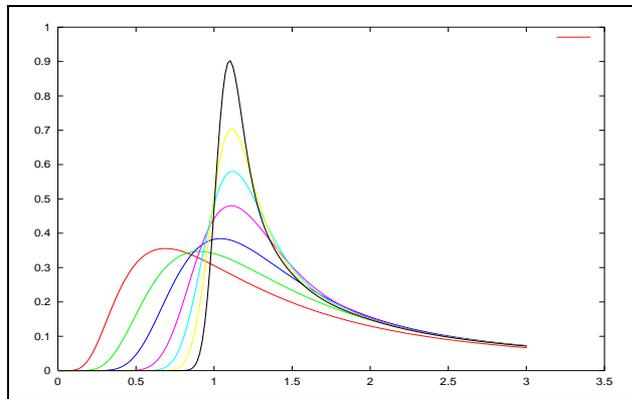


FIG. 5.3. Scaled BTC with 0.1 days pulse input, for $\alpha_L/L = 0.2, 0.1, 0.05, 0.02, 0.01, 0.005$ and 0.002 .

at time $t = 0$ is given for two different time-space steps. In the upper part we have $\tau = 0.05$ days with $M = 200$ for the v partition, and in the lower part $\tau = 0.1$ days with $M = 400$. The numerical dispersion is clearly under control. Indeed, the theoretical response is $T_r = 6.466$ days (see (5.1)), and in the bottom right figure we see breakthrough starting after 6.15 days, with $C_0/2$ after 6.36 days, and maximum C_0 value after 6.60 days.

5.2. Experiment 2. To compare with [W-G], we use the same data as in the first experiment §5.1, but for different values of the longitudinal dispersivity over length, α_L/L , for this determines the shape of the BTC. Results are obtained in the 80×400 grid with $\tau = 0.1$ day. In Fig. 5.2, we give the BTC for a step input of the tracer. In Fig. 5.3 for a pulse input of tracer C_0 during 0.1 days. The figures have been scaled to make comparison to [W-G] possible. For this scaling the maximum of the BTC for $\alpha_L/L = 0.002$ with pulse input has been used, because this curve is the closest to the pure advection case of the previous experiment. This maximum occurred after 6.775 days.

A careful analysis of the figures shows that for low values of α_L/L (≤ 0.02), our scheme produces BTC's like those in [W-G].

REFERENCES

- [B] J. Bear, *Dynamics of Fluid in Porous Media*, Elsevier, New York, 1972.
- [C-K] D. Constales, J. Kačur, Parameter identification by means of dual-well tests, *submitted*.
- [C-M] M.G. Crandall, A. Majda, The method of fractional steps for conservation laws, *Numer. Math.*, **34**:285-314, 1980.
- [G-C] L.W. Gelhar, M.A. Collins, General analysis of longitudinal dispersion in nonuniform flow, *Water Resour. Res.*, **7**:1511-1521, 1971.
- [G-B] D.B. Grove, W.A. Beetem, Porosity and dispersion constant calculations for a fractured carbonate aquifer using the two-well tracer method, *Water Resour. Res.*, **17**:128-134, 1971.
- [H] H.M. Haitjema, *Analytic Element Modeling of Groundwater Flow*, Academic Press, San Diego, 1995.
- [K-L] K.H. Karlsen, K.-A. Lie, An unconditionally stable splitting for a class of nonlinear parabolic equations, *IMA J. Numer. Anal.*, **19**(4):609-635, 1999.
- [P] S.V. Patankar, *Numerical heat transfer and fluid flow*, Hemisphere, Washington (D.C.), 1980. *IMA J. Numer. Anal.*, **19**(4):609-635, 1999.
- [W-G] C. Welly, L.W. Gelhar, Evaluation of longitudinal dispersivity from nonuniform flow tracer tests, *Journal of Hydrology*, **153**:71-102, 1971.

Acknowledgement. The work was funded by the project BOF/GOA 120515 98 of Ghent University. The second autor was also supported by MSM 260 100001 and GACR 201/00/0557.